Topology, Phase Instabilities, and Wetting of Microemulsion Networks

T. Tlusty,[1] S. A. Safran,[1] and R. Strey[2]
[1]*Department of Materials and Interfaces, The Weizmann Institute of Science, Rehovot 76100, Israel*
[2]*Institut für Physikalische Chemie, Luxemburger Strasse 116, D-50939 Köln, Germany*
(Received 16 August 1999)

We predict theoretically the gradual formation of fluctuating, connected microemulsion networks from disconnected globules as the spontaneous curvature is varied, in agreement with recent direct measurements of these topological transitions. The connectivity induced instability together with emulsification failure of the network relate the ultralow tensions and wetting transition to the changing microstructure.

PACS numbers: 64.75.+g, 68.10.Cr, 82.70.–y

The interplay between structural energy and entropy that characterizes the self-assembly of microemulsions (ME) leads to an extremely rich variety of geometries. Among these, the multiply connected sponge, in which the water and oil domains are both continuous, has been extensively studied [1]. These bicontinuous structures are observed around the inversion temperature, $\bar{T}$, where the mean curvature of the surfactant film vanishes. In the very same region, ME systematically exhibit striking thermodynamic features, especially the critical, reentrant two-phase separation and the subsequent formation of a three-phase region [2], where the ME is composed of a surfactant-rich lens that generally wets the interface between the water-rich and oil-rich phases only partially [3]. The behavior of the ultralow tensions at these three interfaces as a function of temperature exhibits a wetting transition, where the lens spreads all over the oil-water interface [4]. Recent experimental studies by Strey and Sottmann on 19 different non-ionic surfactant ME have shown that both the phase diagrams [5] and tensions [6] obey similar universal scaling properties.

Previous theories [7] that focused on the symmetric sponge, where the amphiphilic random interface has equal probabilities to curve towards oil or water, could not reproduce the critical, reentrant phase behavior nor the subsequent criticality near the three-phase region. Motivated by the unexplained reentrance phenomena, we proposed a model for ME based on thermally fluctuating *asymmetric* bicontinuous networks, whose building blocks are cylinders interconnected by junctions [8]. The cylinders are stabilized by the finite spontaneous curvature, c_0, above or below $\bar{T}$ [9]. Recently, these networks with their three-fold "Y-like" junctions have been directly observed by transmission electron microscopy (TEM) [10] (Fig. 1a).

In this paper, we show how a unified explanation of the connection between microstructure and interfacial properties naturally emerges from the fluctuating network model. It consistently predicts the topological transitions of the ME with decreasing spontaneous curvature, c_0 (which is controlled by temperature in non-ionic systems): The ME evolves from spherical globules to long cylinders of radius R that subsequently interconnect by threefold junction, leading to the formation of the bicontinuous network. We introduce the concept of emulsification failure (EF) of networks that allows for the optimization of the *local* curvature energy through rejection of the excess internal phase. In the region of the reentrant phase separation the

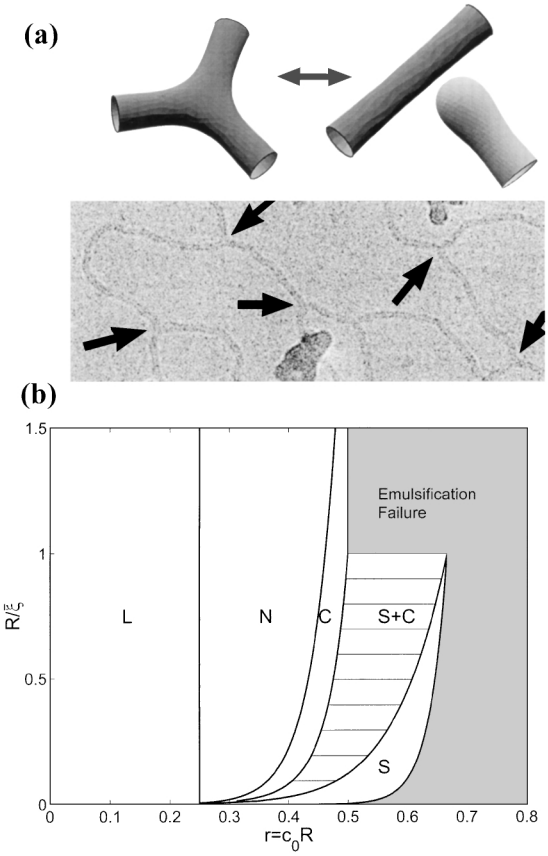

FIG. 1. (a) The formation of a threefold "Y-like" junction. The theoretical shape of the junction, as calculated by numerical minimization, has a lamellar core, while the cylinder terminates with an enlarged spherical end cap. The cryo-TEM image of the Habon G system shows the semiflexible network formed by such junctions [A. B. Grosswasser and Y. Talmon (to be published)]. (b) The phase stability diagram of spheres (S), cylinders (C), lamellae (L), and the network (N) made of interconnected cylinders. Note the series of topological transitions, S → S + C → C → N as c_0R decreases.

 0031-9007/00/84(6)/1244(4)$15.00

global, large-scale network topology is optimized via adjustment of the typical distance, L, between its junctions. The appearance of the three-phase coexistence of ME with almost pure oil and water phases, when the EF and the reentrance loops overlap, therefore signifies the capability of the system to simultaneously tune its structure on *both local and global* length scales. We trace the progression of the microstructure from the curvature-governed dilute network, $L \gg R \sim c_0^{-1}$, to the strong fluctuation regime, where the typical distance between junctions is comparable with their size, $c_0^{-1} \gg L \sim R$, and they form a dense sponge. We predict the consequent dependence on c_0 of the interfacial tension and the resulting wetting transition in agreement with experiment.

We first discuss the sequence of topological transitions that ME show on the way to the formation of bicontinuous networks. At high spontaneous curvature, far from $\bar{T}$ (lower part of the phase diagram in Fig. 1b), one can neglect the thermal fluctuations. The dominant contribution to the free energy (per unit volume) is the local elastic curvature energy, $f_e = \phi r^{-3} E(r)$, where ϕ is the volume fraction of the inner phase (oil or water), $r = c_0 R$ is the ratio of the radius to the optimal radius of curvature; $E(r)$ is the scale invariant curvature energy. Previous studies have dealt with the details of the phase diagram in this regime and we describe only the main results [9]: In a single phase, the radius is determined by the volume to surface ratio $R = 2\delta(\phi/\phi_s)$, where the volume fraction of the surfactant is ϕ_s and δ is the surfactant chain length (R is the cylinder radius, 2/3 of the sphere radius). The curvature energy of cylinders is $E_c(r) = \kappa(1 - 4r)$, where κ is the bending modulus. For spheres, the curvature energy, $E_s(r) = \frac{8}{9}[2\kappa(1 - 3r) + \bar{\kappa}]$, includes a topological contribution proportional to the saddle-splay modulus, $\bar{\kappa}$ (E_s and E_c are measured relative to the curvature energy of lamellae $E_l = 0$). Comparing the energies of the three possible local geometries, one finds that lamellae are optimal in the symmetric regime $r < \frac{1}{4}$ (Fig. 1b). As r increases, there occurs a transition to cylinders, followed by a transition to a region where they coexist with spheres, and finally to a pure phase of spheres. When r is further increased, the free energy becomes unstable with respect to the EF phase separation: In this type of instability the *local* curvature energy, E, is optimized by the rejection of the excess, internal phase to optimize the curvature energy and still obey the geometrical constraints set by composition [11,12]. Coexistence with an excess phase takes place when the osmotic pressure of the material outside the globules vanishes. Expressed in the free energy $f(r, \phi)$, this condition takes the form

$$f + (1 - \phi)\partial_\phi f + (r/\phi)\partial_r f = 0, \qquad (1)$$

or in the scaled form of the curvature energy, $r\partial_r E = 2E$.

The global structure of the ME, and especially the *connectivity* transition from separate cylinders to the bicontinuous network [13], is governed by thermal fluctuations. The cylindrical local geometry [9] is determined by the relatively large curvature energy while all other scales are governed by the smaller free energy of fluctuations, ranging from the stringlike undulation of the branches to the longer wavelength translational entropy of the junctions [8]. To estimate the free energy, consider the network formed when the cylindrical branches are interconnected by z-fold junctions that each cost an energy ϵ (relative to the cylinders) due to their curvature. The junctions behave as an ideal gas of defects in the sense that the entropy is $k_B T$ per junction. The connectivity of the network implies that the number density of junctions, ρ_z, scales nonlinearly with ϕ, the network volume fraction, $\rho_z \sim \phi^{z/2} e^{-\epsilon}$ [14] resulting in an effective attraction (for $z \geq 3$). For disconnected cylinders ($z = 1$), the ideal gas of junctions is replaced by a gas of end caps of number density ρ_1 that each cost curvature energy ϵ_1. This attraction between the junctions is the driving force leading to the connectivity transition from cylinders to network around the line $\rho_3 = \rho_1$. Apart from a logarithmic correction, this transition occurs when the energies of both defects are equal, $\epsilon - \epsilon_1 \simeq \ln\phi$. Figure 1a describes the creation of a junction by the fusion of an end cap and a cylinder with the topological cost of one handle; its contribution to the integral over the Gaussian curvature is $\bar{\kappa} \int K\, dS = -4\pi\bar{\kappa}$. The difference in the mean curvature contribution to the elastic energy, as calculated by numerical or variational minimization, scales approximately linearly with r, $2\kappa \int dS\,(H - c_0)^2 \simeq 4\pi\kappa(Pr - Q)$, with $P \simeq 2.14$ and $Q \simeq 1.04$ [15]. Junctions are optimal for small values of the normalized spontaneous curvature due to their flat lamellar core, while end caps are preferred at larger r by their spherical cap (Fig. 1a). The resulting transition line,

$$r_n = \frac{1}{P}\left(Q + \frac{\bar{\kappa}}{\kappa} + \frac{1}{4\pi\kappa}\ln\phi\right), \qquad (2)$$

is depicted in Fig. 1b. We include the effects of short wavelength fluctuations by the renormalized bending modulus $\kappa(R) = -(\alpha/4\pi)\ln(R/\xi)$, and saddle-splay modulus $\bar{\kappa}(R) = (\bar{\alpha}/4\pi)\ln(R/\bar{\xi})$; the corresponding membrane thermal persistence lengths are $\xi = \delta\exp(4\pi\kappa_0/\alpha)$ and $\bar{\xi} = \delta\exp(-4\pi\bar{\kappa}_0/\bar{\alpha})$, where κ_0 and $\bar{\kappa}_0$ are the bare values of the moduli and the exponents are $\alpha = 3$, $\bar{\alpha} = \frac{10}{3}$ [16]. As the temperature approaches the inversion temperature, $\bar{T}$, the curvature determined length scale increases as $R \sim 1/c_0 \sim 1/|T - \bar{T}|$, and $\bar{\kappa}$ increases logarithmically from its typical negative nominal value, $\bar{\kappa}_0 < 0$. This leads to the expansion of the network region (Fig. 1b), since higher values of $\bar{\kappa}$ favor the saddlelike shape of the junction [17]. This theoretical prediction for the topological transition, spheres $\rightarrow$ spheres + cylinders $\rightarrow$ cylinders $\rightarrow$ network, was recently substantiated by direct cryo-TEM measurements of non-ionic ME [10].

We also anticipate that the network will be unstable with respect to EF similar to that of globules. Motivated by the experimental phase diagrams, which exhibit straight, constant-r EF lines, we neglect the small effect of the entropic contribution in the free energy of the network and substitute in Eq. (1) only the dominant curvature contribution, $\phi r^{-3} E_c(r)$. Since this local energy is not sensitive to connectivity, we obtain an identical result for both disconnected cylinders and networks for the optimal radius,

$$c_0 R_c = \frac{2\ln(R_c/\xi) - 1}{4\ln(R_c/\xi) - 1}. \quad (3)$$

R_c has two limits; the curvature-governed regime ($h = c_0\xi \ll 1$), shown in Fig. 1b, $R_c = 1/(2c_0)$, while in the entropy-governed regime ($h \sim 1$) it crosses over to $R_c \sim \xi$. The suggested EF of cylinders followed by EF of networks, at lower values of c_0 (Fig. 1b), is in accord with experiment [10].

Apart from the local EF instability, which is also common to globules, the bicontinuous network exhibits a unique instability which directly results from its global connectivity: The entropic part of the free energy is unstable to phase separation when the effective attraction, $-\rho_z \sim -\phi^{z/2} e^{-\epsilon}$, overcomes the repulsion. This occurs for values of the junction energy lower than a critical value. Since $\phi^{z/2}$ represents an effective attraction only if the exponent is higher than linear (or $z \geq 3$), we find that this type of phase separation is unique to the connected structures. Within the network picture, the reentrant phase separation loops and the subsequent three-phase coexistence emerge as direct results of the nonmonotonic behavior of the junction energy, $\epsilon(r)$ [8]. The curvature energy of the junction exhibits a minimal value at r_* [15] which corresponds to a steep maximum of the attraction $\sim e^{-\epsilon}$. When the maximal attraction exceeds a critical value, the ME phase separates into two networks of the same cylindrical radius r, which differ in the density of junctions, as verified by experiment [10]. In the phase diagram, this *global* instability is manifested by the appearance of a two-phase coexistence loop bounded by two critical points with a width that expands as $\Delta r = |r - r_*| \sim (1 - h/h_*)^{1/2}$ [8] (h_* refers to the double critical points where the loops first appear).

As T approaches the inversion temperature, $\bar{T}$ (where $h = c_0 = 0$), the loops expand until the increasing radius of their cylinders make the networks unstable to the local EF [Eq. (3)], and they reject the excess phase. The consequent three-phase coexistence between two ME networks, dense and dilute, together with an excess phase, is therefore the outcome of the simultaneous action of two distinct mechanisms for phase separation [12]; the local EF is characterized by the radius of curvature, R_c [Eq. (3)], and governs the coexistence of the network with its excess phase, while the global attraction of the junctions is characterized by the typical junction-junction correlation length and governs the two-network coexistence. The experimental phase diagrams [6] and tension curves [5] of many non-ionic ME systems, in both the two-phase and three-phase temperature regimes, exhibit a universal data collapse. We suggest that the source of this universality is purely geometrical; it is the connectivity of the ME network that provides an inherent, material independent, topological mechanism for attraction. Recent cryo-TEM experiments [10] which prove our structural understanding of the three-phase region, have also confirmed this theoretical proposal that indeed the bicontinuity is sustained even up to the highly asymmetric regime where the reentrant phase separation first occurs.

In the emulsification failure (EF) scenario, the macroscopic interface between the ME and the excess phase is a well-defined monolayer [18]. For this case, the experimentally measurable, macroscopic interfacial tension, σ, is simply the free energy per unit area required to unfold a segment of the ME network to a planar monolayer when the surfactant molecules are transferred to the newly formed interface. Far from $\bar{T}$ ($h \gg 1$), the dominant contribution is the elastic energy of the flattened interface due to the difference between its curvature energy and the optimal value at the network EF. This scales as $\kappa(R)c_0^2$ and therefore vanishes at $\bar{T}$. An additional contribution to the interfacial tension, which dominates in the strong fluctuation regime, accounts for the loss of network entropy, and this contribution determines the finite, ultralow value of the tensions at $\bar{T}$, where the curvature contribution vanishes. To estimate σ we employ an expansion of the reentrance loop and the EF around the critical end points $h = h_3 \simeq 0.9$, where the three-phase body first appears, with respect to the critical parameter $\Delta h = 1 - |h|/h_3$ [8]. The resulting values for the interfacial tensions between the two networks and their excess phase are (in units of $k_B T \xi^{-2}$)

$$\sigma_{\pm}(h) = \kappa(R_c)h^2 + (\xi/R_c)^2(A \pm B\Delta h^{1/2}), \quad (4)$$

where the constants $A \simeq 0.4$ and $B \simeq 0.02$ are found by expansion of the network free energy. The higher value, σ_+, corresponds to the dilute network phase, due to its higher entropy (weaker repulsion forces), and the lower value, σ_-, corresponds to the dense ME phase. In Fig. 2 the experimental curves $\sigma_+(h)$ measured for 19 ternary systems [6] collapse onto the universal theoretical prediction of Eq. (4), when normalized by $k_B T \xi^{-2}$, where ξ was independently measured by small-angle neutron scattering (SANS) [19]. The data shows an asymptotic h^2 behavior with a deep decrease, over 3 orders of magnitude, to the ultralow nonvanishing value $A + B \simeq 0.42$ at the entropy-governed symmetric sponge.

By contrast, when the two coexisting phases are both networks, the corresponding interface is a continuous transition layer separating regions where the branches have the same radius but their local density (or the density of junctions) differs. Near the critical end point where the two networks merge, the thickness of this transition layer

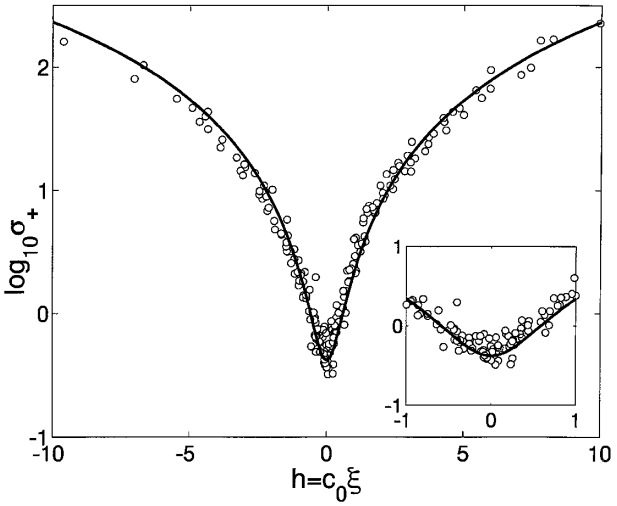

FIG. 2. The tension at the interface between the dilute network and the excess phase, σ_+, of 19 non-ionic microemulsions [6] collapse onto the scaling result (4) when plotted in units of $k_B T \bar{\xi}^{-2}$, where $\bar{\xi}$ was measured independently by SANS [19]. The data crosses over from the curvature governed regime, $h \gg 1$, to the ultralow nonvanishing value at the symmetric sponge, $h \ll 1$ (inset).

increases. Recalling that the phase separation is along constant-r tie lines, we consider only inhomogeneities of the network volume fraction by adding a term proportional to the square of its local gradient, $(\nabla\phi)^2$. Within a mean-field approximation, this approach yields an interfacial tension that vanishes as $\sigma_c \sim \Delta h^{3/2}$ at the critical points. Following the experiments, we assume that the boundary crosses over from a monolayer to a continuous transition layer in the vicinity of $\bar{T}$ ($h \ll 1$), where the thickness of the interface is comparable to the radius of the cylinders, $\sigma_- = \sigma_c$ [18]. This is typical of the symmetric sponge, where the global length scale becomes comparable to the size of the domains. The resulting tension takes the following form:

$$\sigma_c(h) = (\bar{\xi}/R_c)^2 (A - B)\Delta h^{3/2}. \tag{5}$$

The consequent balance of the three surface forces, given by Eqs. (4) and (5), determines the wetting properties of the ME: A generalized Young's law implies that the contact angle of a nonwetting lens [3] of the dense network phase floating between the dilute network and the excess phase is $\cos\theta = (\sigma_+^2 - \sigma_-^2 - \sigma_c^2)/(2\sigma_c\sigma_-)$. The tensions of the symmetric sponge at $h = 0$ are almost equal $\sigma_+ \simeq \sigma_- = \sigma_c$, and the theory predicts a lens with a contact angle $\theta \simeq 2\pi/3 - 4B/\sqrt{3}A \simeq 0.63\pi$. As the ME becomes asymmetric and approaches the critical end points, $h = h_3$, the tension between the merging phases vanishes as $\sigma_c \sim \Delta h^{3/2}$, which is faster than the vanishing of the difference between the tensions at the monolayers separating these phases and the excess phase, that scales as $\sigma_+ - \sigma_- \sim \Delta h^{1/2}$. Consequently, close enough to the critical end points, it is energetically favorable to avoid creating an interface between the dilute network and the excess phase by spreading an intervening layer of the dense network phase. Consistent with experiment [4], we predict a wetting transition at the points, $h = h_W$, which are defined by the complete wetting condition, $\sigma_+ = \sigma_- + \sigma_c$, leading to $h_W/h_3 \simeq 1 - 2B/A \simeq 0.9$. In this vicinity the theory predicts that the contact angle vanishes as $\theta \sim (h_W - h)^{1/2}$. We note that the entropic residue of the free energy due to the thermal fluctuations of the network is essential to obtain this wetting transition as well as the ultralow nonvanishing tensions at $\bar{T}$.

The authors thank T. Sottmann, who collaborated in the measurements, and K. Brakke and U. Schwarz for their help in using the SURFACE EVOLVER software. We are indebted to A. Bernheim-Grosswasser and Y. Talmon for generously allowing us to use the micrograph. We are grateful to the Israel Science Foundation Center for Self-Assembly and the Minerva Gerhard Schmidt Center.

[1] *Micelles, Membranes and Microemulsions and Monolayers*, edited by W. M. Gelbart, A. Ben-Shaul, and D. Roux (Springer-Verlag, Berlin, 1994).
[2] M. Kahlweit, R. Strey, and G. Busse, J. Phys. Chem. **94**, 3881 (1990).
[3] B. Widom, Langmuir **3**, 12 (1987).
[4] M. Aratono and M. Kahlweit, J. Chem. Phys. **95**, 8578 (1991); M. Kahlweit, R. Strey, and G. Busse, Phys. Rev. E **47**, 4197 (1993).
[5] T. Sottmann and R. Strey, J. Chem. Phys. **106**, 8606 (1997).
[6] T. Sottmann and R. Strey, J. Phys. Condens. Matter **8**, A39 (1996).
[7] G. Gompper and M. Schick, *Self-Assembling Amphiphilic Systems* (Academic, New York, 1994).
[8] T. Tlusty, S. A. Safran, R. Menes, and R. Strey, Phys. Rev. Lett. **78**, 2616 (1997).
[9] S. A. Safran, L. A. Turkevich, and P. A. Pincus, J. Phys. (Paris), Lett. **45**, 19 (1984).
[10] A. Bernheim-Grosswasser, T. Tlusty, S. A. Safran, and Y. Talmon, Langmuir **15**, 5448 (1999).
[11] M. S. Leaver and U. Olsson, Langmuir **10**, 3449 (1994).
[12] S. A. Safran and L. A. Turkevich, Phys. Rev. Lett. **50**, 1930 (1983).
[13] Y. Bohbot, A. Ben-Shaul, R. Granek, and W. M. Gelbart, J. Chem. Phys. **103**, 8764 (1995).
[14] T. J. Drye and M. E. Cates, J. Chem. Phys. **96**, 1367 (1992).
[15] T. Tlusty and S. A. Safran, J. Phys. Condens. Matter **12**, 253 (2000).
[16] F. David, in *Statistical Mechanics of Membranes and Surfaces*, edited by D. Nelson, T. Piran, and S. Weinberg (World Scientific, Singapore, 1989).
[17] D. C. Morse, Phys. Rev. E **50**, R2423 (1994); L. Golubović, Phys. Rev. E **50**, R2419 (1994).
[18] D. Langevin and J. Meunier, in *Micelles, Membranes and Microemulsions and Monolayers* (Ref. [1]).
[19] T. Sottmann, R. Strey, and S.-H. Chen, J. Chem. Phys. **106**, 6483 (1997).